Research article

Journal of RAMAN SPECTROSCOPY

Received: 5 December 2014 Revised: 5 February 2015 Accepted: 7 February 2015 Published online in Wiley Online Library: 8 March 2015

(wileyonlinelibrary.com) DOI 10.1002/jrs.4673

Subsurface analysis of painted sculptures and plasters using micrometre-scale spatially offset Raman spectroscopy (micro-SORS)

Claudia Conti,[a]* Chiara Colombo,[a] Marco Realini[a] and Pavel Matousek[b]*

A recently developed variant of spatially offset Raman spectroscopy (SORS) for the non-invasive analysis of thin painted layers, micro-SORS, has been applied, for the first time, to real objects of Cultural Heritage – namely painted sculptures and plasters. Thin layers of paint originating from multiple restoration processes often applied over many centuries have been analysed non-destructively using micro-SORS to depths inaccessible to, or unresolvable into separate layers, by conventional confocal Raman microscopy. The concept has been demonstrated on several artistic artefacts of historical significance originating from Italy and dating from the medieval to the 18th century. The technique extends the depth applicability of Raman spectroscopy and with its inherently high chemical specificity that expands the portfolio of existing non-destructive analytical tools in Cultural Heritage permitting to avoid cross-sectional analysis often necessitated with this type of samples with conventional Raman microscopy. Currently, the method is non-invasive only for artworks that can be placed under Raman microscope although there is a prospect for its use in a mobile system with largely removed restrictions on sample dimensions. © 2015 The Authors *Journal of Raman Spectroscopy* Published by John Wiley & Sons Ltd.

Keywords: spatially offset Raman spectroscopy; subsurface; non-destructive; sculptures; plasters

Introduction

Chemically specific analysis of painted multilayers by non-destructive and non-invasive means is a topical issue in the field of Cultural Heritage. This capability is in part fulfilled by confocal Raman microscopy. However, this method is applicable mainly to (near) surfaces of painted layers, a limitation stemming from depth-resolving power of the technique restricted to depths at which sample is transparent or semi-transparent. As paint layers are highly diffusely scattering, the restriction can be very severe and often to depths of only several micrometres. This limitation often necessitates obtaining a sample by invasive and destructive means, e.g. by taking a small fragment and analysing its cross section (e.g. using confocal Raman microscopy[1,2]), a solution that is highly undesirable and in many cases impossible with precious objects of art. Consequently, there is a strong need for non-invasive analysis applicable to deeper subsurface layers, which are beyond the reach of conventional confocal Raman microscopy. Recently, a new approach for non-invasive probing in turbid (diffusely scattering) media has been proposed and demonstrated on artificially painted layers: micro-spatially offset Raman spectroscopy (micro-SORS).[3] At the moment, this method is non-invasive only for the artworks that can be placed under the microscope objective. The method is non-destructive, allowing the analysis of the sublayers without any particular sample preparation. The technique derives its sublayer-resolving properties from its parent technique SORS,[4–6] which would be capable of probing through thin painted layers but would be unable to resolve them into separate layers. In contrast, micro-SORS permits their resolution into separate layers.

In its basic form, micro-SORS relies on collecting at least two Raman spectra using a Raman microscope; the first one with sample in a conventional 'imaged' position and the second with sample in a 'defocused' position, attained by moving the sample away from microscope objective by a 'defocusing distance Δz'.[7] The sample displacement from the 'imaged' position causes the defocusing of both laser illumination and Raman collection zones on sample surface (Fig. 1). The former measurement, in the 'imaged' position, yields a spectrum dominated by the surface layer and corresponds, in effect, to a zero spatially offset measurement in conventional SORS analysis. The latter measurement, in the 'defocused' position, yields a Raman spectrum, which has a significantly higher degree of relative signal contribution from sublayers[7] and corresponds to a non-zero spatially offset acquisition in conventional SORS.

Using scaled subtraction of the 'imaged' Raman spectrum from the 'defocused' spectrum aiming at cancelling the contributions from the surface layer, one can recover the pure Raman spectrum of sublayer. The pure Raman spectrum of the surface layer can in turn be obtained in analogy by a reverse process – by scaled

* *Correspondence to: Claudia Conti, Consiglio Nazionale delle Ricerche, Istituto per la Conservazione e la Valorizzazione dei Beni Culturali (ICVBC), Via Cozzi 53, Milano 20125, Italy.*
E-mail: c.conti@icvbc.cnr.it
* *Correspondence to: Pavel Matousek, Central Laser Facility, Research Complex at Harwell, STFC Rutherford Appleton Laboratory, Harwell Oxford OX11 0QX, UK.*
E-mail: pavel.matousek@stfc.ac.uk

Consiglio Nazionale delle Ricerche, Istituto per la Conservazione e la Valorizzazione dei Beni Culturali (ICVBC), Via Cozzi 53, Milano 20125, Italy

Central Laser Facility, Research Complex at Harwell, STFC Rutherford Appleton Laboratory, Harwell Oxford OX11 0QX, UK

Journal of RAMAN SPECTROSCOPY

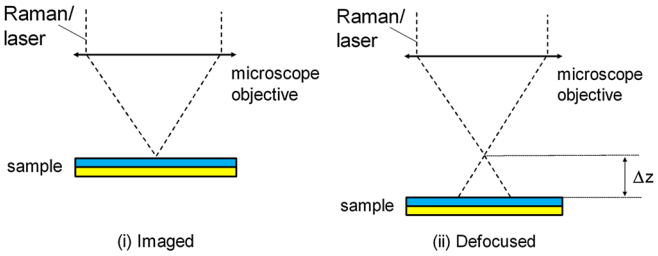

Figure 1. Schematic diagram of experimental geometries in micro-spatially offset Raman spectroscopy analysis. Measurements are taken (i) with the sample in 'imaged' and (ii) 'defocused' positions. The latter realised by moving the sample away from microscope objective by displacement *z* from the 'imaged' position. (This figure is available in colour online at wileyonlinelibrary.com/journal/jrs.)

subtraction of the 'defocused' spectrum away from the 'imaged' spectrum cancelling any subsurface features present.

As the Raman signal at the 'imaged' position is typically stronger than that in the 'defocused' position, the 'defocused' measurement can be conveniently boosted by using longer acquisition times or higher laser powers. The latter permitted by the laser spot size on sample surface being considerably larger than that in the 'defocused' position.

For a three-layer system, the measurement of three different sample positions Δz is required, and several subtractions need to be performed to cancel contributions from non-desired layers.

In this work, we apply the micro-SORS concept, for the first time, to real objects of Cultural Heritage demonstrating its performance on painted sculptures and plasters.

Experimental

Specimens

The polychrome sculptures originate from prestigious devotional places called 'Sacred Mounts' (United Nations Educational, Scientific and Cultural Organization World Heritage sites) constructed during the late 15th and 17th centuries in North Italy as a consequence of the counter-reformation. They consist of a series of chapels containing wall paintings and terracotta or stucco sculptures representing the life of Christ (such as Varallo Sacred Mount) or the Mysteries of the Rosary (e.g. Varese and Ossuccio Sacred

Figure 2. Polychrome sculpture images: (S1) Christ and (S2) the sleeping man, Ossuccio Sacred Mount; (S3) Christ's disciple, Varese Sacred Mount; and (S4) St Joseph, Varallo Sacred Mount. The white circles indicate the investigated areas. (This figure is available in colour online at wileyonlinelibrary.com/journal/jrs.)

Table 1. Investigated samples

Artistic site	Artwork	Area	Label
Ossuccio Sacred Mount (Como)	Stucco sculpture, Christ	Blue mantle	S1
Ossuccio Sacred Mount (Como)	Stucco sculpture, sleeping man	Yellow garment	S2
Varese Sacred Mount (Varese)	Terracotta sculpture, Christ's disciple	Red mantle	S3
Varallo Sacred Mount (Vercelli)	Terracotta sculpture, St Joseph	Green mantle	S4
Masegra Castle (Sondrio)	Painted plaster	Yellow	S5

Mounts). In this paper, we report micro-SORS results that we consider to be the most representative of the data we gathered; in Fig. 2, the sculptures and their relative analysed areas are shown.

As also reported in Table 1, besides the four samples chosen as exemplars of polychrome sculptures, one sample of painted plaster originates from the medieval Masegra Castle (Sondrio). Small fragments were taken from the artworks and analysed both using micro-SORS (intact and without any preparation) and using conventional confocal Raman microscopy (using cross-sectional analysis).

Raman spectroscopy

The analyses have been carried out using a Senterra dispersive micro-Raman spectrometer (Bruker) with a 1200 grooves per millimetre grating and coupled to an Olympus BX51 microscope equipped with 20× and 50× objectives. The laser excitation wavelength was 785 nm with a power at the sample of ~10 mW. The Raman spectra were acquired using a Peltier cooled CCD detector (1024 × 256 pixels).

In the micro-SORS measurements, a 50 μm circular pinhole was used to acquire the 'imaged' spectra to provide extra discriminating capability. The 'defocused' spectra were collected without the pinhole with only a spectrograph 50 × 1000 μm slit. The 'imaged' spectra were acquired with 50-s acquisition time (five accumulations and 10 s each) and the 'defocused' spectra with an overall acquisition time ranging from 100 to 300 s (five accumulations with 20–60 s each). After the acquisition of the 'imaged' spectrum, the motorised stage was moved away from the microscope objective over a range of a few tens of micrometres to several millimetres.

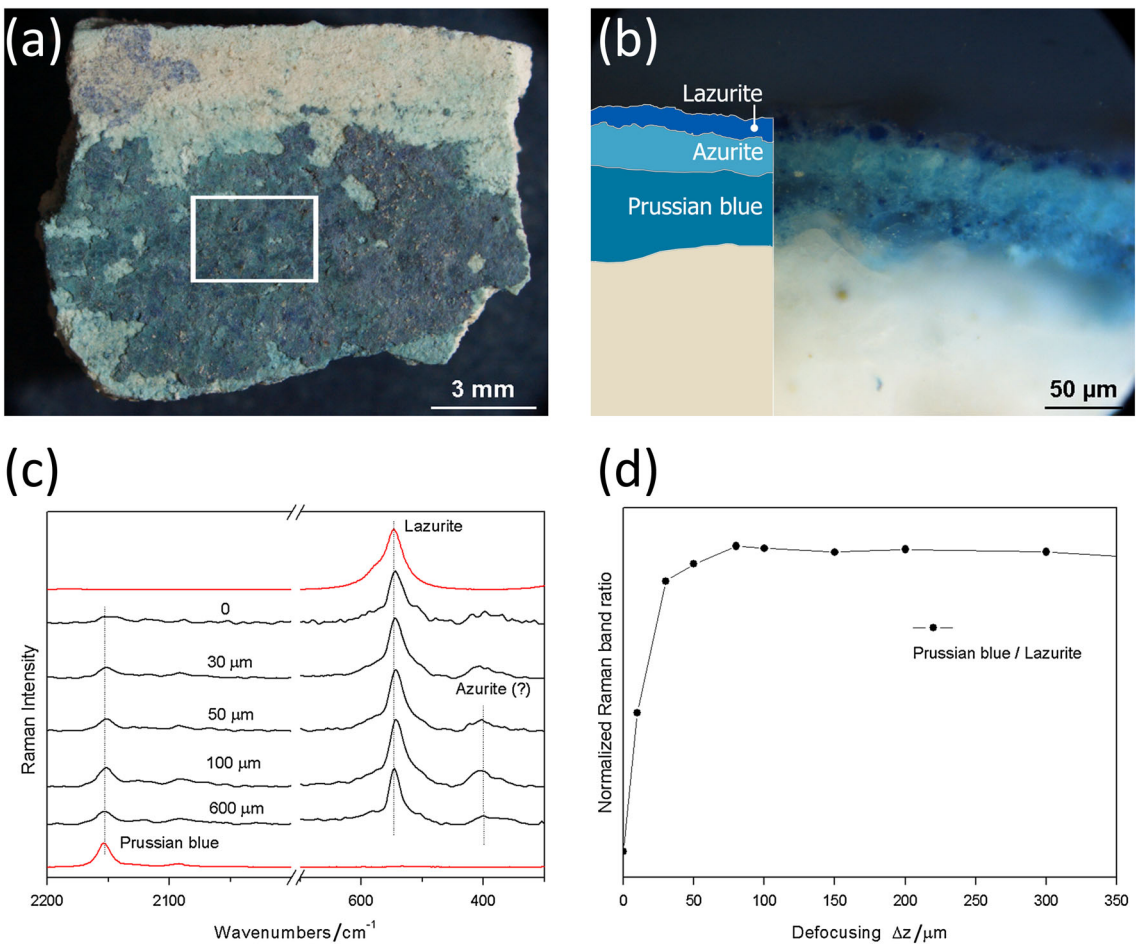

Figure 3. S1 sample: (a) fragment image (the white square indicates the area analysed with micro-spatially offset Raman spectroscopy); (b) optical image and scheme of the stratigraphy; (c) the defocused spectra are shown for different distances from the 'imaged' plane indicated next to each spectrum (0 = 'imaged' position). The spectra are offset for clarity. Note that the line markers are for guidance to emphasise the changing relative intensity of lazurite and Prussian blue with the defocusing distance; the reference spectra are acquired on sample cross section using conventional Raman spectroscopy; and (d) Raman intensity ratio (Prussian blue/lazurite) of the spectra acquired at different defocusing distances Δz. (This figure is available in colour online at wileyonlinelibrary.com/journal/jrs.)

Optical microscopy

Microscopic observations have been carried out in reflected light using a Leitz Ortholux microscope with Ultropack illuminator equipped with a digital image capturing system.

Results and discussion

The first demonstration of the use of micro-SORS on real objects of art was carried out on a stucco statue. A small sample fragment was acquired from a blue mantle of Christ (S1) (Fig. 3). An inspection carried out using an optical microscope of sample cross section reveals the presence of three blue layers: the external one, approximately 20-μm thick containing well-defined blue particles; the middle one consisting of a homogeneous light blue material being 20-μm thick; and the most deepest, a 30-μm thick layer containing small blue particles. A conventional Raman microscopy carried out on the cross section over individual layers enabled to infer the composition of blue pigments; the external layer exhibits a very characteristic line of ultramarine blue (lazurite) identified through its marker Raman band at ~549 cm^{-1} assigned to the symmetric stretching mode of the S_3^- ions in a sodium alumino–silicate matrix.[8] The middle layer consists of azurite, the basic copper(II) carbonate exhibiting the most intense Raman band at 401 cm^{-1} and finally the blue particles of the third layer evidenced through a characteristic Raman signature of the iron(III) hexacyanoferrate(II) called Prussian blue at ~2153 cm^{-1}. This pigment has been introduced in the early 17th century[9]; thus, its presence gives an indication of *post quem* these blue areas were painted.

Figure 3(c) shows the results of micro-SORS defocusing measurements performed on this blue fragment. The Raman spectrum in the 'imaged' position ('0') is dominated by contribution from the top layer, lazurite, although traces of azurite and Prussian blue cannot be completely excluded. As the sample is displaced from its 'imaged' position and moved farther away from the microscope objective, the contribution of the most internal layer relative to the surface layer increases dramatically, while that of the middle layer is rather negligible, in line with expectations. The lack of information obtained from the middle layer can be explained by the relative weakness of Raman cross section of azurite compared with that of the other two pigments. The Raman intensity ratio of the spectra acquired at different defocusing distances Δz considering the most intense bands of Prussian blue (2153 cm^{-1}) and lazurite (549 cm^{-1}) is shown in Fig. 3(d). Even though lazurite persists up to the largest defocusing distance used, the band intensity ratio changes, and the presence of Prussian blue as a separate (deeper) layer (rather than blended with lazurite in a single layer) is ascertained.

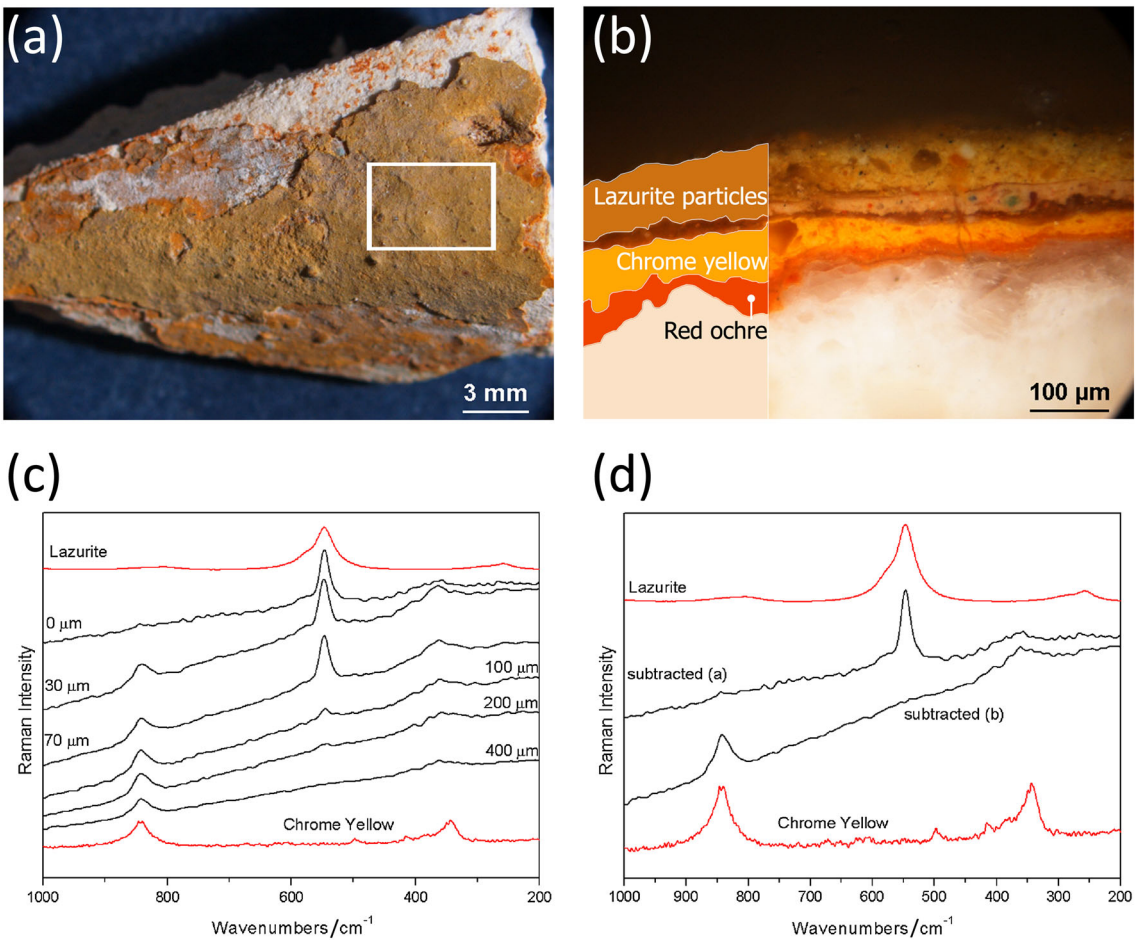

Figure 4. S2 sample: (a) fragment image (the white square indicates the area analysed with micro-spatially offset Raman spectroscopy); (b) optical image and scheme of the stratigraphy; (c) the defocused spectra are shown for different distances from the imaged plane indicated next to each spectrum (0 = 'imaged' position). The spectra are offset for clarity; and (d) the numerical recovery of pure Raman spectra of individual layers. The top and the bottom spectra are reference spectra of pure lazurite and chrome yellow pigments, respectively, obtained in separate measurements on sample cross section using conventional Raman spectroscopy. Recovered Raman spectra of (a) the top layer and (b) sublayer using a scaled subtraction of 400-μm and 0-μm spectra. The spectra are offset for clarity. (This figure is available in colour online at wileyonlinelibrary.com/journal/jrs.)

In another example, a fragment overpainted with dark yellow pigment was used (S2). Micro-Raman analysis on a sample cross section using conventional confocal Raman instrument coupled with optical microscopy reveals the presence of three layers (Fig. 4(b)): the external one (100-μm thick) consisting of yellow ochre and lazurite, the latter used traditionally to give a dark hue to the mantle; the thickness of the second layer is rather inhomogeneous, ranging from 20 to 70 μm, and its yellow colour originates from a chrome yellow pigment [lead(II) chromate], clearly distinguishable by two very intense peaks at 842 and 361 cm^{-1}; and the last and more internal layer (from 10-μm to 40-μm thick) is red in appearance stemming from the presence of red ochre.

Micro-SORS measurements on this sample have been carried out starting from a blue particle of the external layer, because of the very low and noisy signal of the yellow portion. Lazurite is the main compound detected in the 'imaged' position with a negligible, almost undetectable presence of 842-cm^{-1} peak of chrome yellow. Moving away from the sample surface, the contribution of chrome yellow strongly increases, and the peak intensity of lazurite dramatically decreases, up to a point where no signal can be visible (Fig. 4 (c)). As for the second and more internal layer, no signal from the red ochre was detected.

The relative intensity change between the top and middle layers with defocusing permits the separation of the spectra into pure components belonging to individual layers by scaled subtraction cancelling the residual peak of the non-targeted layer as described earlier. To illustrate this process, we have recovered the pure Raman spectrum of the top layer by subtracting the defocused spectrum from the 'imaged' Raman spectrum using a scaling factor set to cancel the residual middle-layer Raman bands that might be present in the zero Raman spectrum. A reverse process, where 'imaged' spectrum is subtracted away from the defocused one cancelling surface contributions, produces a pure Raman spectrum of sublayer. The result of this analysis where the estimates of pure Raman spectra of individual layers are produced by this approach is shown in Fig. 4(d). The resulting pure components of individual layers compare well with reference spectra shown for each layer permitting the identification of layer paint types in the sample by this non-destructive subsurface method.

The red mantle of one of Christ's disciples (S3) has been repainted many times during the centuries; thus, its stratigraphy is characterised by many overlapped red layers composed by different red pigments (red lake, red lead, red ochre and cinnabar). As revealed by cross-sectional analysis (Fig. 5(b)), the external layer (100–120-μm thick) consists of red lead [dilead(II) lead(IV) oxide], with two very sharp peaks near 122 and 550 cm^{-1}. In a sublayer, cinnabar [α-mercury(II) sulfide] is used as a red pigment, with three very characteristic Raman bands at 253, 286 and 342 cm^{-1}, the first and most intense band arising from ν(HgS) mode.[10] Between these two layers, a very thin and discontinuous layer of red ochre has been detected.

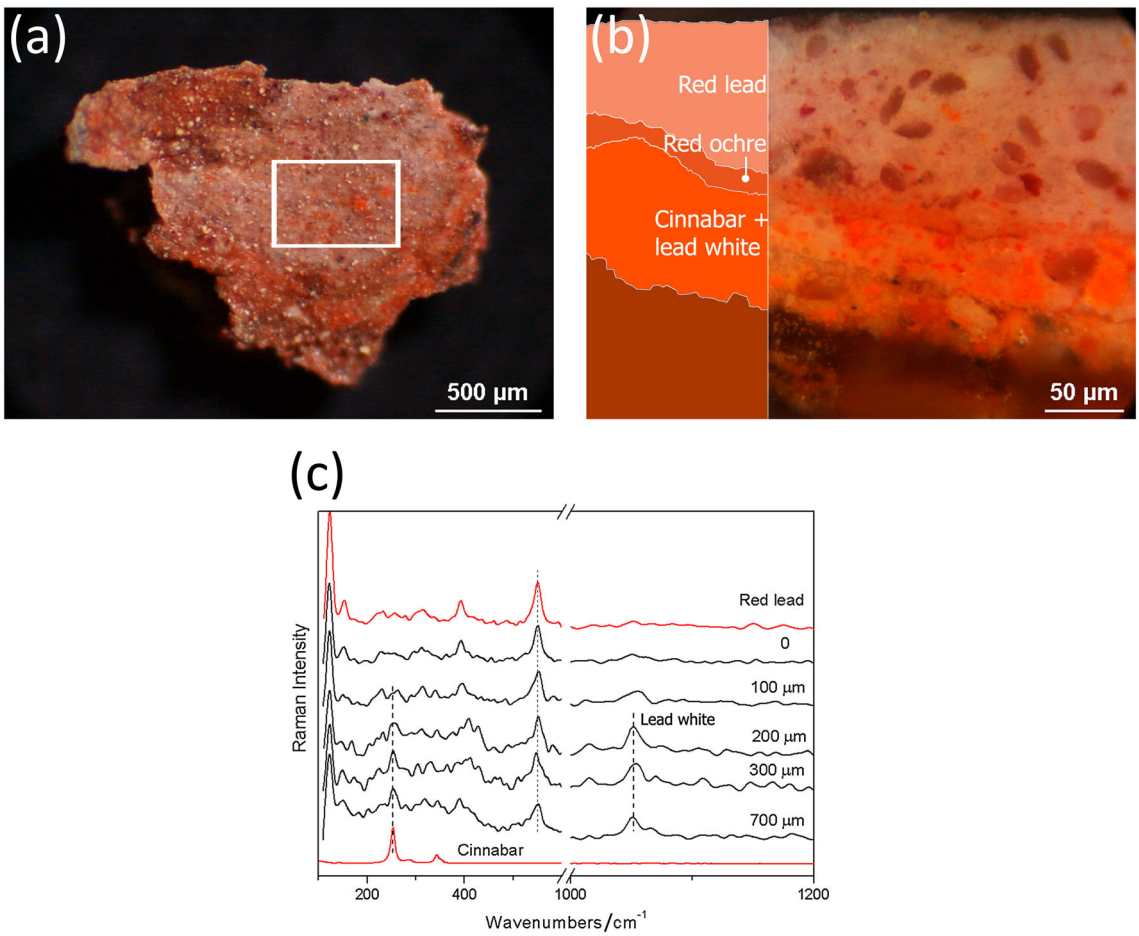

Figure 5. S3 sample: (a) fragment image (the white square indicates the area analysed with micro-spatially offset Raman spectroscopy); (b) optical image and scheme of the stratigraphy; and (c) the defocused spectra are shown for different distances from the imaged plane indicated next to each spectrum (0 = 'imaged' position). The spectra are offset for clarity. Note that the line markers are for guidance to emphasise the changing relative intensity of the red lead, cinnabar and lead white with defocusing. The reference spectra are acquired on sample cross section using conventional Raman spectroscopy. (This figure is available in colour online at wileyonlinelibrary.com/journal/jrs.)

Although the micro-SORS Raman spectra are noisier than in previous examples, they still exhibit distinct features of the pigments present both in the surface and in the depth, permitting their unequivocal identification (Fig. 5(c)). No Raman peaks of red ochre from the thin intermediate layer have been observed. The 'imaged' position spectrum exhibits only red lead Raman bands, but with the increase of the defocusing distance, the relative contribution of cinnabar arises together with lead white (basic lead carbonate – 1051 cm^{-1}) used as an extender of cinnabar pigment.

The St Joseph green mantle (S4) shows a very complex stratigraphy with almost 20 distinct layers and a large number of different pigments present; moreover, this sculpture also shows strong signs of decay. The pigments used for the first green layer, deduced by the cross-sectional analysis, are Prussian blue mixed with chrome yellow and barium white (barium sulfate), one of the most used white pigment (Fig. 6). The 'imaged' spectrum shows the presence of two very common decay products, gypsum (calcium sulfate dihydrate – 1008 cm^{-1}) and anglesite [lead(II) sulfate – 977 cm^{-1}]. As the sample is displaced from its 'imaged' position, the characteristic line at 989 cm^{-1} of barium white arises; on the contrary, gypsum and anglesite rapidly decrease (Fig. 6). As the cross-sectional analysis revealed the presence of barium white only in the first layer, it is clear that the decay affects only the most superficial portion of the stratigraphy; in fact, the decay product bands (gypsum) decrease when those of barium white increase.

In the course of the study, we have also identified a notable limitation of micro-SORS associated with samples possessing very high heterogeneity. A micro-SORS measurement carried out on another location on the surface of this sample (Fig. 5(d)) showed only a random fluctuation of Raman intensity of anglesite and barium white upon defocusing (as opposed to just monotonous decrease or increase). This anomalous behaviour has been attributed to highly heterogeneous surface of this sample; the larger the illumination and collection area, the higher the number of particles that was sampled and averaged. This phenomenon needs to be considered when measuring highly inhomogeneous samples such as decayed surfaces.

Whether the change of the relative intensity of Raman bands is due to the depth resolution of micro-SORS or an artefact of surface inhomogeneity could be tested by first performing a surface area scan in 'imaged' position to ascertain the degree of homogeneity/heterogeneity of the probed area and comparing its level with the magnitude of evolution of signals upon defocusing. Additional limitations of the method include potential inapplicability to highly absorbing and highly fluorescing layers, extremely thin interlayers or sublayers and pigments with low Raman cross sections.

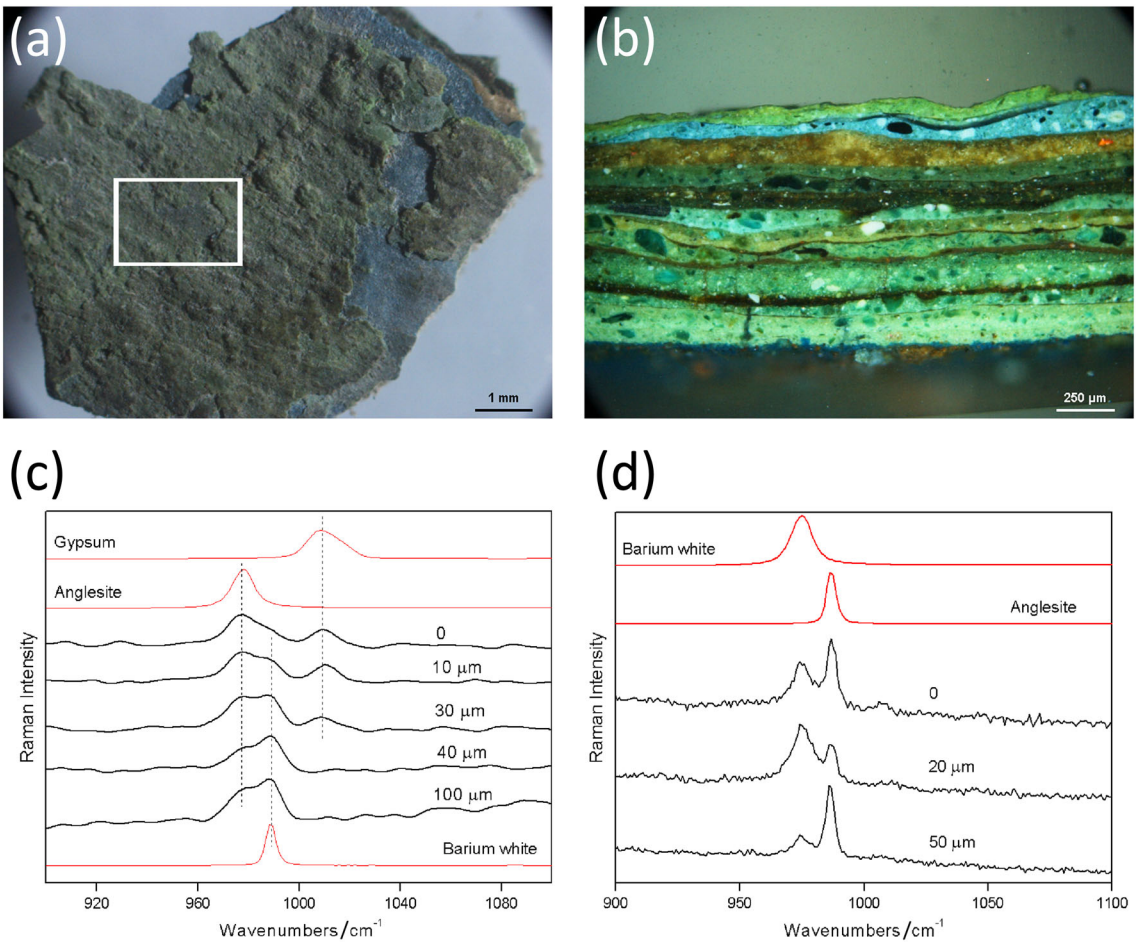

Figure 6. S4 sample: (a) fragment image (the white square indicates the area analysed with micro-spatially offset Raman spectroscopy); (b) optical image; (c) the defocused spectra are shown for different distances from the imaged plane indicated next to each spectrum (0 = 'imaged' position). The spectra are offset for clarity. Note that the line markers are for guidance to emphasise the changing relative intensity of the anglesite, gypsum and barium white with defocusing. The reference spectra are acquired on sample cross section using conventional Raman spectroscopy; and (d) an anomalous (random) dependence of Raman intensity of anglesite and barium white on defocusing stemming from excessively heterogeneous sample surface. (This figure is available in colour online at wileyonlinelibrary.com/journal/jrs.)

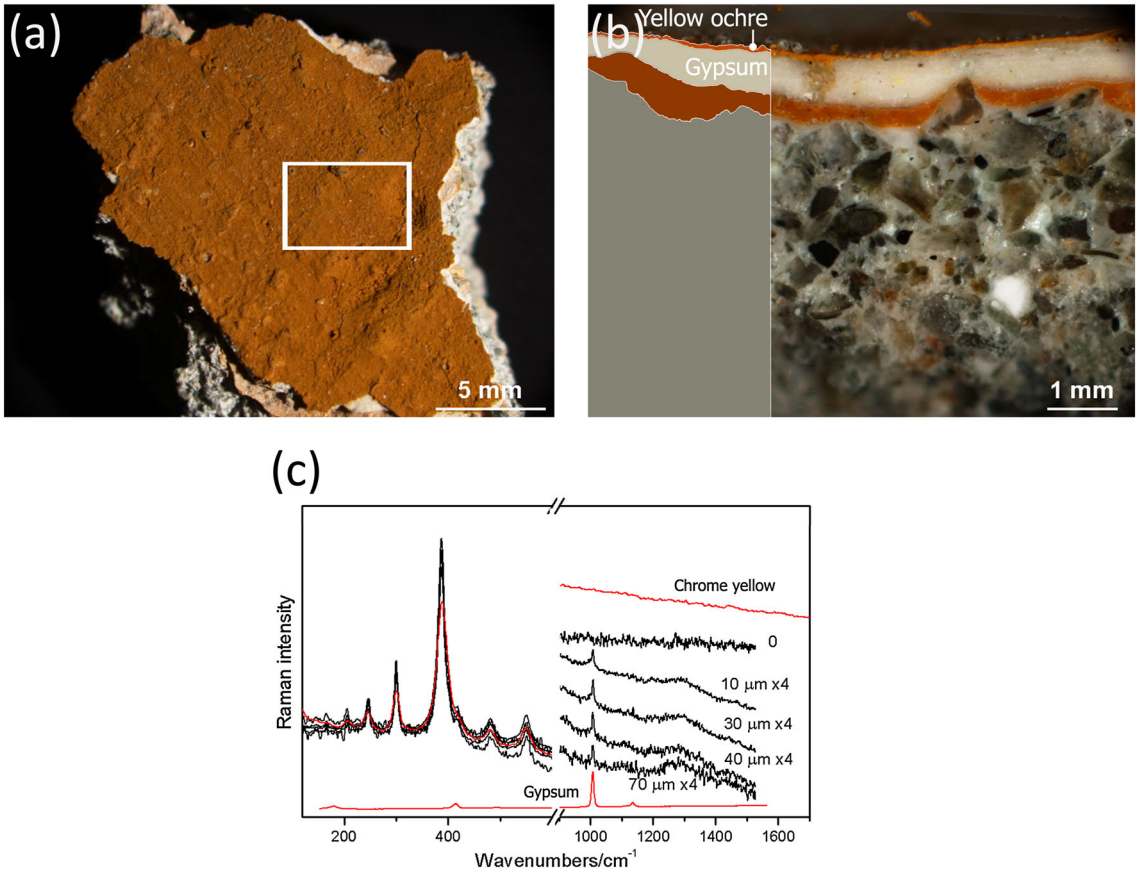

Figure 7. S5 sample: (a) fragment image (the white square indicates the area analysed with micro-spatially offset Raman spectroscopy); (b) optical image and scheme of the stratigraphy; and (c) the defocused spectra are shown for different distances from the imaged plane indicated next to each spectrum (0 = 'imaged' position). Because of the large difference in Raman cross sections between the yellow ochre and gypsum bands, different scales have been applied to the spectra for clarity. The reference spectra are acquired on sample cross section using conventional Raman spectroscopy. (This figure is available in colour online at wileyonlinelibrary.com/journal/jrs.)

The last example presented here is a plaster painted with a yellow pigment (Fig. 7). Conventional analysis reveals the presence of three distinct layers on top of this plaster. Micro-SORS measurements allowed to distinguish clearly the first two layers; the external one, yellow, a few tens micrometres thick and composed of yellow ochre and the second one, approximately 500-μm thick, showing white colour due to the presence of gypsum. The Raman spectrum in the 'imaged' position was dominated by contribution from the top layer, namely yellow ochre. As the sample was displaced from its 'imaged' position, the contribution of the most internal layer increased revealing the hidden presence of gypsum. The measurements have been repeated at different points on sample surface, and at each point, a very similar evolution was observed. In general, the occurrence of gypsum can be ascribed to the presence of a white layer or to a decay process involving the inner portions of the material. The reproducibility of the micro-SORS results indicates a relatively homogeneous distribution of gypsum inside the surface that points out to the presence of an intentionally painted layer, made of gypsum, or, alternatively, a strongly decayed layer.

Conclusions

Several examples of non-destructive analysis of painted layers on painted sculptures and plasters using micro-SORS have been given revealing the chemical makeup of upmost layers. The technique is also completely non-invasive for those artworks that can be placed under the microscope objective, thus expanding the portfolio of available non-invasive/non-destructive analytical tools in Cultural Heritage. Moreover, the method has a potential for being developed into a portable totally non-invasive analytical tool.

Acknowledgement

We would like to thank Dr Fabio Bevilacqua for the opportunity to study the Ossuccio Sacred Mount statuary.

References

[1] L. R. Čukovska, B. Minčeva–Šukarova, A. Lluveras-Tenorio, A. Andreotti, M. P. Colombini, I. Nastova *J. Raman Spectrosc.* **2012**, *43*, 1685.
[2] P. Westlake, P. Siozos, A. Philippidis, C. Apostolaki, B. Derham, A. Terlixi, V. Perdikatsis, R. Jones, D. Anglos *Anal. Bioanal. Chem.* **2012**, *402*, 1413.
[3] C. Conti, C. Colombo, M. Realini, G. Zerbi, P. Matousek *Appl. Spectrosc.* **2014**, *68*, 686.
[4] P. Matousek, I. P. Clark, E. R. C. Draper, M. D. Morris, A. E. Goodship, N. Everall, M. Towrie, W. F. Finney, A. W. Parker *Appl. Spectrosc.* **2005**, *59*, 393.
[5] P. Matousek, M. D. Morris, N. Everall, I. P. Clark, M. Towrie, E. Draper, A. Goodship, A. W. Parker *Appl. Spectrosc.* **2005**, *59*, 1485.
[6] K. Buckley, P. Matousek *Analyst* **2011**, *136*, 3039.
[7] C. Eliasson, M. Claybourn, P. Matousek *Appl. Spectrosc.* **2007**, *61*, 1123.
[8] I. M. Bell, R. J. H. Clark, P. J. Gibbs *Spectrochim Acta A* **1997**, *53*, 2159.
[9] L. Burgio, R. J. H. Clark *Spectrochim Acta A* **2001**, *57*, 1491.
[10] R. L. Frost, H. G. M. Edwards, L. Duong, J. T. Kloprogge, W. N. Martens *Analyst* **2002**, *127*, 293.